A study of the impact of stau mixing on the chargino limits

K. Jakobs, J.Vollinga
Institut für Physik, Universität Mainz

May 25, 2000

Abstract

In the present note the impact of stau mixing on the chargino exclusion limits in the MSSM is studied. The ALEPH data collected at various center-of-mass energies in the range between 189 and 202 GeV have been used. The standard two- and three body chargino analyses have been performed together with a search for chargino decays via sleptons. The effects of mixing are studied in detail for several values of $\tan\beta$ and μ. Exclusion limits in the $(m_{\tilde{\nu}}, M_{\tilde{\chi}^{\pm}})$-plane as well as limits on the mass of charginos are given as a function of the mixing angle φ_{τ}.

1 Introduction

In the MSSM, where the sleptons and sneutrinos are generally the lightest SUSY partners of fermions, there are three principle decay modes of the chargino. The relative importance of these depends on the parameters and of the mass hierarchy of the SUSY model. A chargino can either decay to a neutralino and a W-boson, to a sneutrino and the corresponding lepton, or to a slepton and the corresponding neutrino. As usual, the decays via a virtual W are referred to as three body and those via a sneutrino as two-body chargino decays. The third decay mode is referred to as slepton decay of the chargino.

Due to the relatively high mass of the tau lepton, mixing between the left- and right-handed staus can be large, modulated by the off-diagonal term in the stau mass matrix, $-M_\tau(A_\tau + \mu \tan\beta)$. The lightest stau, $\tilde{\tau}_1$, can be significantly lighter than the other sleptons and the sneutrinos, causing an increase in the branching ratio of charginos to final states with taus. In addition, the decay amplitude depends on the field content of the chargino, and it is most enhanced in the gaugino region.

In the present note the effects of stau mixing on the chargino limits are studied. The standard three- and two-body chargino analyses are performed and combined with an analysis searching for chargino decays via sleptons. These decays become important for small values of m_0 and for large mixing angles. In order to increase the sensitivity for large stau mixing a special tau-tau analysis has been developed [1].

In the case of three-body chargino decays, the various analyses searching for different final states have been combined. The optimal combination has been determined as a function of ΔM, the mass difference between the decaying chargino and the lightest neutralino, BR_{lep}, the branching ratio of the chargino to leptons (e, μ and τ) and of P_τ, the probablity for the lepton being a tau.

In Section 2 of the present note the selections used, including the tau-tau selection, are briefly described. This includes a discussion on the determination of the optimal combination as a function of ΔM, BR_{lep} and P_τ for three body chargino decays. In Section 3 chargino limits in the standard (μ, M_2)-plane are given for different m_0 values for the no-mixing case. The phenomenology of stau mixing and the relevant parameters are briefly introduced in Section 4. The final exclusion limits are given in Section 5 in the $(m_{\tilde{\nu}}, M_{\tilde{\chi}^\pm})$-plane as a function of the stau mixing angle φ_τ for various values of $\tan\beta$.

2 Chargino selections

If stau mixing effects are considered, the lightest stau may become the lightest slepton and tau-tau final states become important. A special selection of hadronic tau decays has been developed, which is briefly described in the following. It should be noted that leptonic decays of taus are included in the standard electron or muon selection. After the description of the tau identification the different chargino decay modes are discussed.

2.1 Tau Identification

The tau selection has been developed in Ref.[1] and [2]. Both an inclusive and a somewhat more exclusive tau selection have been defined. In the inclusive hadronic tau selection one- and three prong tau decay candiates are selected with relatively loose cuts on the tracks. To get a cleaner tau sample, intermediate ρ and a_1 states in the tau decay chain are reconstructed. These selections will be referred to as *loose* and *tight* tau selections respectively in the following.

The tau selection starts by applying the Durham jet algorithm [6] in such a way that all particles in the event are forced into two jet clusters. Since tau jets appear to be narrow, only those tracks are considered further that are within a cone with an opening angle of 18° around the jet axis. For lower energy jet clusters the opening angle is enlarged and is and is given by $\arccos(1 - 2\ m_{jet}^2/E_{jet}^2)$, where m_{jet} and E_{jet} are the mass and the energy of the jet. For a tau candidate the following requirements have to be fulfilled:

- Either one or three charged tracks are reconstructed in the defined cone around the jet axis. In the case where three tracks are found, the total charge has to be ± 1. A candidate is also kept if two tracks are found in the cone and one of them is identified as an electron. Such an event might be interpreted as an asymmetric conversion for which only one leg has been reconstructed.
- The visible mass, computed from objects in the cone, has to be smaller than 2 GeV.
- The so-called cluster radius r_{clus}, defined as the ratio between the longitudial momentum of the energy flow objects with respect to the jet axis and their total momentum, has to be larger than $min\ \{0.98, (1 - 0.8\ m_{jet}^2/E_{jet}^2)\}$

A jet candiate passing these criteria is considered to be identified as a *loose* tau. In order to be classified as *tight* tau, one of the following exclusive channels has to be reconstructed:

- Decay via a ρ meson: $\tau^- \to \rho^- \nu_\tau \to \pi^- \pi^0 \nu_\tau$
  It is required that there is only one charged track and one or two additional neutral clusters in the cone. The reconstructed visible mass in the cone has to be in a window of $\pm$ 300 MeV around the ρ mass. If only one neutral cluster is identified, it is assumed that the two photons from the π^0 decay have not been resolved. In this case the π^0 mass is assigned to the neutral cluster in the invariant mass calculation.

- Three prong decay via an a_1 meson: $\tau^- \to a_1^- \nu_\tau \to \pi^- \pi^+ \pi^- \nu_\tau$
  It is required that there are exactly three charged tracks and no additional neutral objects in the cone. The reconstructed mass has to be in a window of $\pm$ 400 MeV around the a_1 mass.

- One prong decay via an a_1 meson: $\tau^- \to a_1^- \nu_\tau \to \pi^- \pi^0 \pi^0 \nu_\tau$
  It is required that there is only one charged track and two to four additional neutral clusters. The reconstructed visible mass computed from objects in the cone has to be in a window of $\pm$ 400 MeV around the a_1 mass. Also in this case, the π^0 mass is assumed in the calculation of the invariant mass, if the π^0 decay products have not been resolved.

2.2 Three body chargino decays

2.2.1 The selections used

If all sfermions are heavier than the chargino, the three body decay mode via W^* exchange is dominant. The W^* decays according to its standard branching ratios to fermion-antifermion pairs, leading via the dominant $q\bar{q}$-decay to four jet final states, which due to the neutralino, are accompanied by missing momentum. The analyses looking for these four jet topologies are referred to as $4J$ analyses. In addition to these dominant four jet decays, also decays into a jet pair, a lepton and the corresponding neutrino are important ($2Jl$-analysis). If sleptons and sneutrinos are heavier than the charginos the double leptonic decay, leading to an acoplanar lepton pair, has only a small branching ratio in the order of 10%.

The $4J$, $2Jl$ and $2J\tau$ selections used in the present analysis are identical to those developed for chargino searches at lower energies [3], [4]. For the higher energies, updated cuts have been implemented [5]. The hadronic analyses have been optimized for various different ΔM regions, such that in total 9 hadronic chargino selections have been included. They are listed together with the leptonic selections in Table 1.

For the leptonic decays the standard $ACOLZ$ and $LLVL$ analyses have been used, again with updated cuts for higher energies. Depending on ΔM a sliding cut on the momentum of the leading lepton has also been applied. For three body decays it has been optimized and parametrized. The basic *ACOLZ* and *LLVL* selection criteria are also applied to select acoplanar tau pairs. In the three body analysis, a combination of hadronic tau pairs is only kept if at least one of the taus is identified as a tight tau. For the tau-tau selection a special optimization of the cuts has again been performed [1]. The optimal cuts have been found to be very close to the ones used in the standard acoplanar lepton selection. Details can be found in Ref.[1].

Table 1 gives an overview on the full list of selections used in the three body analysis. It is also indicated for what regions of ΔM the various selections have been optimized. Out of the 14 different selections listed here the $ll - L$ and $l\tau - L$ selections have been combined in the calculation of the optimal combination (see below).

optimized for	4-jet	2-jet-l	2-jet-τ	$\tau - \tau$	l-τ	l-l
very small Δm	4J-VL	2Jl-VL				
small Δm	4J-L	2Jl-L	2Jτ-L		$l\tau$-L	ll-L
large Δm	4J-H	2Jl-H	2Jτ-H	$\tau\tau$	$l\tau$-H	ll-H
very large Δm			2Jτ-VH			

Table 1: *Summary of the various analyses used in the three body chargino search; the region for which the various analyses have been optimized is also indicated.*

2.2.2 The optimal combination

At each point of the SUSY parameter space the optimal combination of the different three body analyses has been determined using the $\bar{N}_{95}$ prescription. This combination depends on the parameters of the SUSY model. In addition to the ΔM dependence, also the branching ratio to leptons (BR_{lep}), and the fraction of leptonic decays into tau leptons (P_τ) has been included. Given the many different selection and the complexity of the BR_{lep} and P_τ dependence, a computer program, called *ARRASTEL*, has been written [1] to compute the optimal combination for each point in parameter space spanned by ΔM, BR_{lep}, and P_τ.

In the ARRASTEL program a scan over the allowed range of ΔM is performed. For each point in ΔM the efficiency for signal events, the expected background and the number of candidates in the data samples have been computed for each of the possible 8192 combinations of the 13 analyses introduced above. Based on these numbers the optimal combination has been determined according to the $\bar{N}_{95}$ prescription. This combination, together with its values of efficiency, background and $\bar{N}_{95}$ is relevant for the ΔM value considered and for the values of BR_{lep} and P_τ as used in the Monte Carlo generation of the signal samples. For other values of BR_{lep} and P_τ the corresponding branching ratios and thereby the efficiencies are scaled according to the following relations:

Topology	Branching Ratio
$4J$	$(1 - BR_{lep})^2$
$2J - \tau$	$2 \cdot BR_{lep}(1 - BR_{lep})\ P_\tau$
$2J - l$	$2 \cdot BR_{lep}(1 - BR_{lep})\ (1 - P_\tau)$
$\tau - \tau$	$BR_{lep}^2\ P_\tau^2$
$l - \tau$	$2 \cdot BR_{lep}^2\ P_\tau\ (1 - P_\tau)$
ll	$BR_{lep}^2\ (1 - P_\tau)^2$

Using these relations, for each point in the $(\Delta M, BR_{lep}, P_\tau)$ parameter space the best combination of analyses has been determined. Maps of efficiencies, backgrounds and candidates are written out for further analysis.

The results of the *ARRASTEL* calculations are shown in Figs.1 and 2. In Fig. 1 those regions of parameter space are indicated where individual analyses are included in the optimal combination. These maps are given as a function of ΔM and BR_{lep} for two different values of P_τ. The maps shown in the upper part of the figure correspond to $P_\tau = 0.35$, which is close to the non-mixing value of 0.33. The maps shown in the lower part have been computed assuming a value of 0.85 for P_τ. It is obvious from these figures that the various analyses are important in those regions of ΔM and BR_{lep} for which they have been designed. It is however also found, that some of the analyses have a certain pick-up efficiency in regions of parameter space where they have not been designed for and a better $\bar{N}_{95}$ is obtained if they are included in the combination.

In Fig. 2 the values for efficiency, background and $\bar{N}_{95}$ are shown for the selected optimal combination, again as a function of ΔM and BR_{lep}, assuming P_τ to be 0.35. As expected, the efficiency and the background level show discontinuities at the switching points of analyses, whereas the $\bar{N}_{95}$ values are found to be continuous by construction.

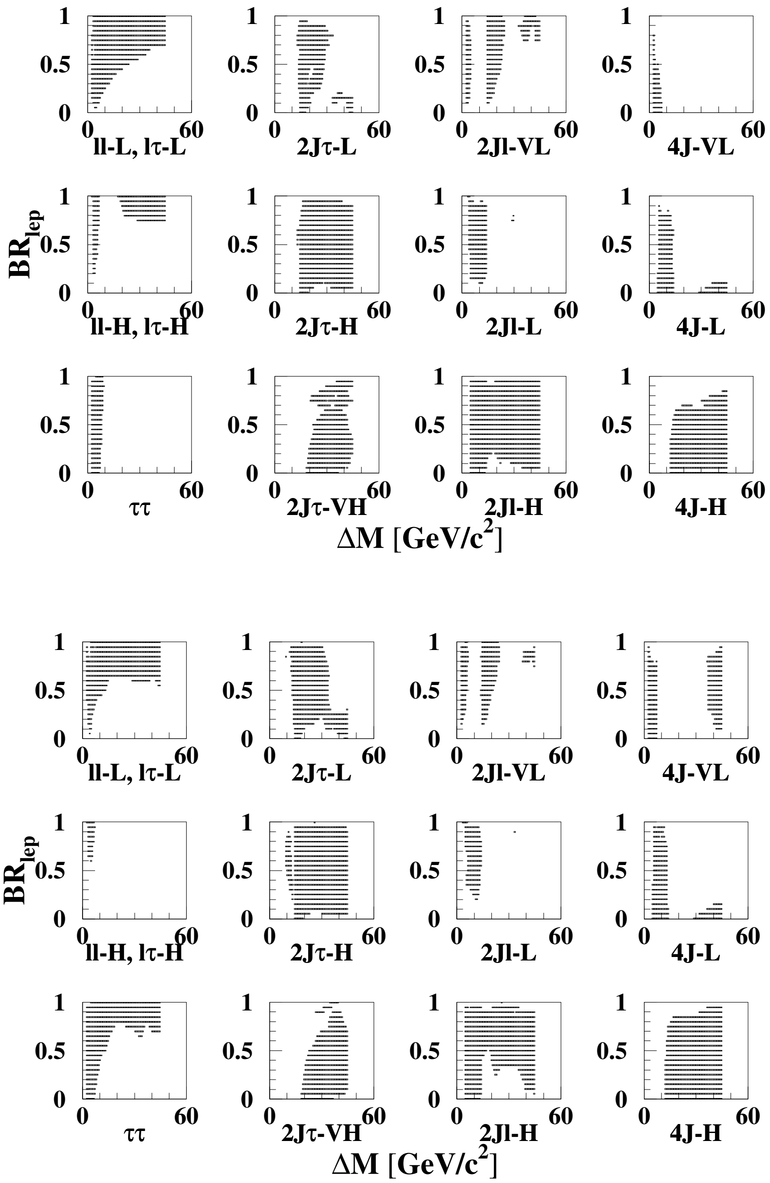

Figure 1: *Maps indicating the regions in ΔM and BR_{lep} space where individual analyses are included in the combination for three body chargino decays. The analyses are included in the marked regions. The parameter P_τ has been fixed to be 0.35 in the upper part and 0.85 in the lower part of the figure.*

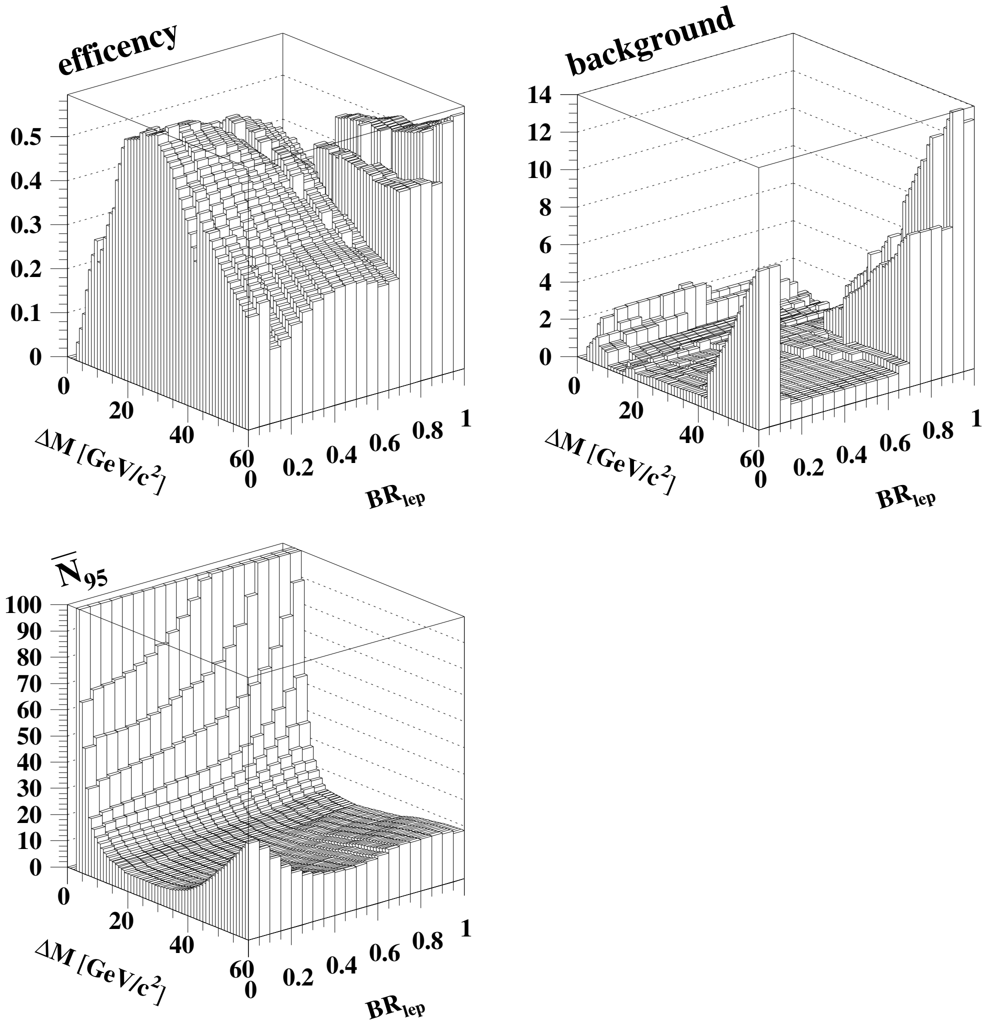

Figure 2: *Efficiency, number of expected background events for the luminosoty corresponding to the 196 GeV data sample and $\bar{N}_{95}$ for the optimal combination, as a function of ΔM and BR_{lep}, for $P_\tau = 0.35$.*

2.3 Two body chargino decays

If sneutrinos are lighter than the charginos, also the two-body decays, $\chi^{\pm} \to l\tilde{\nu}$, become kinematically allowed. For the two body chargino decays the standard $ACOLZ$ and $LLVL$ analyses have been used, again with updated cuts for higher energies. The transition point between these two analyses has been optimzed using the $\bar{N}_{95}$ prescription. It has been found to be around 13 GeV, relatively independent of the centre-of-mass energy. Depending on ΔM a sliding cut on the momentum of the leading lepton has also been applied, which in this case can be calculated from the masses of the particles involved.

2.4 Chargino decays via sleptons

As mentioned above, the slepton decay mode, $\chi^{\pm} \to \tilde{l}\nu \to l\chi^0\nu$, becomes dominant for small m_0 values or for large stau-mixing. In the case of stau mixing the fraction of tau decays increases significantly. Therefore, a special analysis has been designed for these decays. Since the final state consists of an acoplanar lepton pair with missing energy, the $ACOLZ$ and $LLVL$ selections have again been used to perform the basic selection.

The efficiencies of these selections have been found to depend primarily on the mass difference ΔM between the decaying slepton and the neutralino. The second mass difference involved, the mass difference Δm between the chargino and the slepton, has been found to be less important. In addition, the efficiencies have been found to be lower for $\tau\tau$ final states than for ee or $\mu\mu$ final states. The efficiencies of the ACOLZ selection for the selectron and smuon decays are shown in Fig.3a) as a function of the mass difference ΔM. The results obtained for various values of Δm are superimposed. The corresponding efficiency curves for chargino decays via staus are shown for comparison in Fig.3b). The energy distribution of the reconstructed leptons depends on the mass differences ΔM and Δm. In Fig.4 the momentum of the leading lepton normalized to the beam energy is shown for several values of ΔM and Δm. In Fig.4a) and b) the distributions are shown for electrons and muons resulting from chargino decays via selectrons and smuons for various combinations of $(\Delta m/\Delta M)$. In Fig.4c) the corresponding distributions are shown for hadronic taus resulting from chargino decays via staus. Again, it can be seen that the lepton momenta depend primarily of the mass difference ΔM. In the case of tau final states a broader energy distribution is found, which is due to the worse energy resolution for reconstructed hadronic tau decays as compared to reconstructed electrons or muons. These distributions can be used to introduce an additional mass dependent cut to discriminate signal against background, which is dominated by WW events. The corresponding shape of the background is shown in Fig.4d).

The optimal cut has been determined as a function of ΔM and Δm for the case

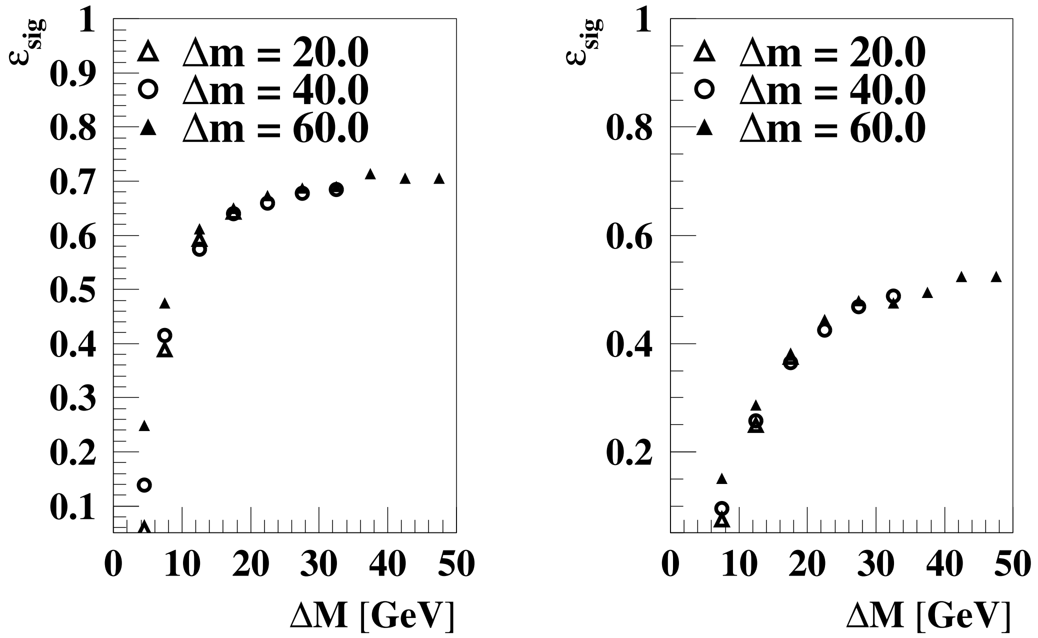

Figure 3: *Efficiency of the* ACOLZ *selection for chargino decays via sleptons as a function of the mass difference* ΔM *between slepton and neutralino for different values of* Δm*, the mass difference between the chargino and the slepton. In plot a) the efficiencies are shown for decays via selectrons and smuons, in plot b) the corresponding values are shown for decays via staus.*

where an electron or a muon is the leading lepton and for the case where a tau is the leading lepton. The results are shown in Fig.5. The optimal cut is found to depend mainly on the mass difference ΔM with an additional somewhat weaker dependence on Δm. These dependences have been parametrized and have been used in the final analysis.

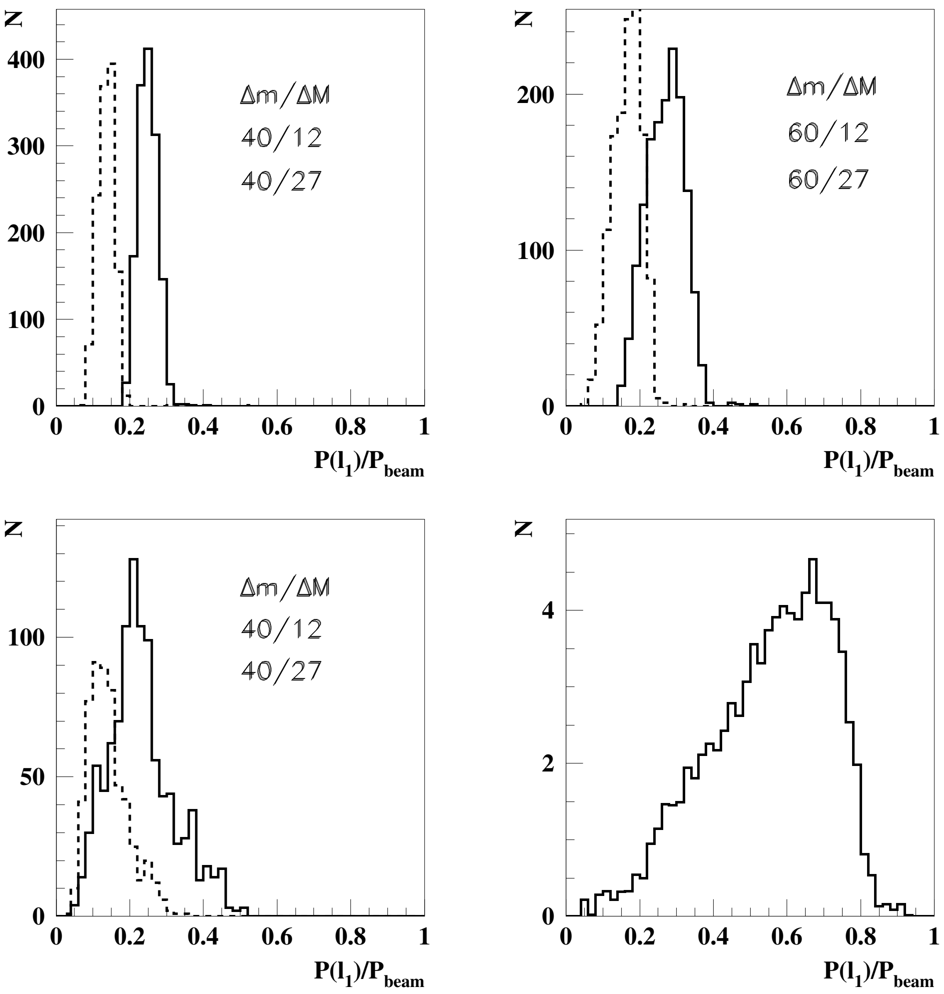

Figure 4: *Momentum of the leading lepton for chargino decays via sleptons normalized to the beam energy for: a),b) selectron and smuon decays for various pairs of (Δm / ΔM)-values, c) stau decays for various pairs of (Δm / ΔM)-values, d) sum of all backgrounds (dominated by WW background).*

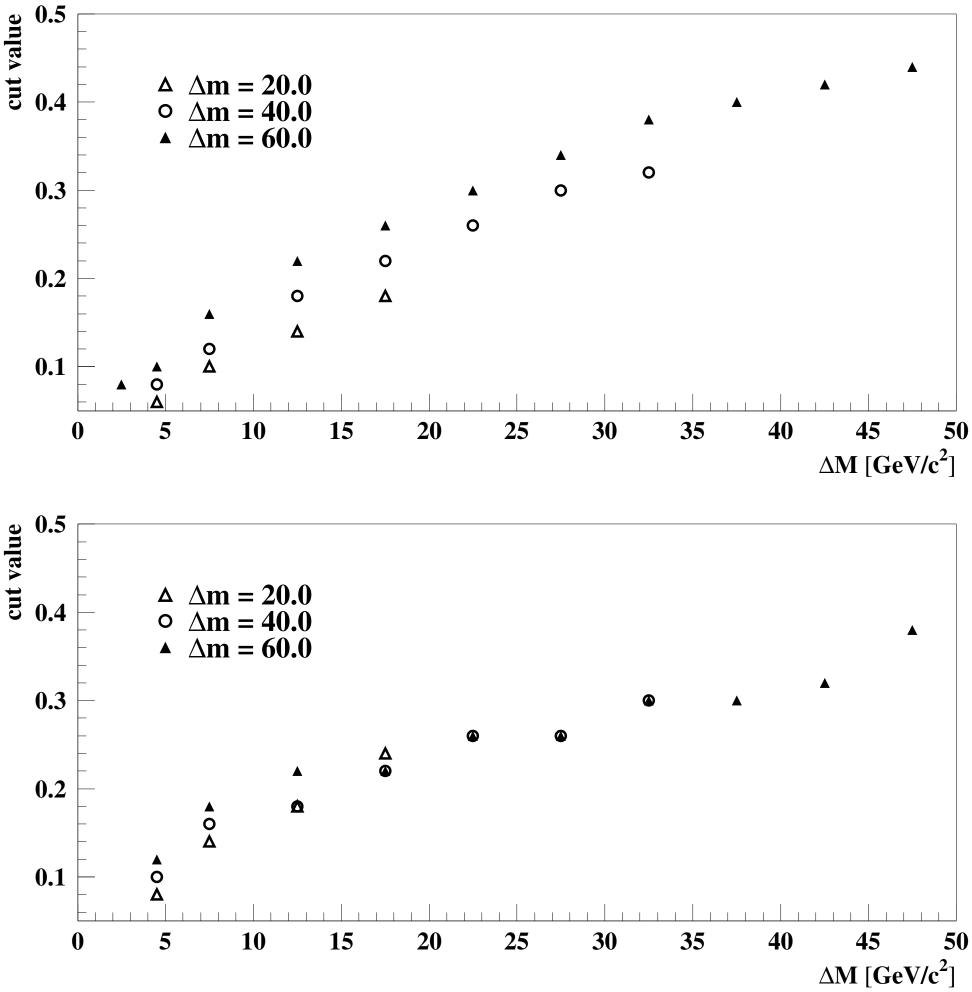

Figure 5: *Optimal cut on the momentum of the leading lepton as a function of ΔM and Δm for selectron and smuon decays (upper plot) and for stau decays (lower plot).*

3 Chargino limits for the no-mixing case

For large values of m_0 ($m_0 >\sim 200$ GeV) sleptons and sneutrinos are heavy and they will not affect the phenomenology of chargino decays at LEP energies. In this case the chargino decays via a virtual W boson. The exclusion limits obtained in the (μ, M_2) plane are shown in Fig.6 for $\tan\beta$ values of 1, 1.4, 2, and 35. The exclusion limits have been based on the analysis of all ALEPH data taken at centre-of-mass energies in the range between 189 and 202 GeV. Also the excluded regions based on LEP-1 data are shown. The kinematic limit for $\sqrt{s} = 202$ GeV is indicated as dashed line. For these large m_0 values this limit can be reached for all $\tan\beta$ values.

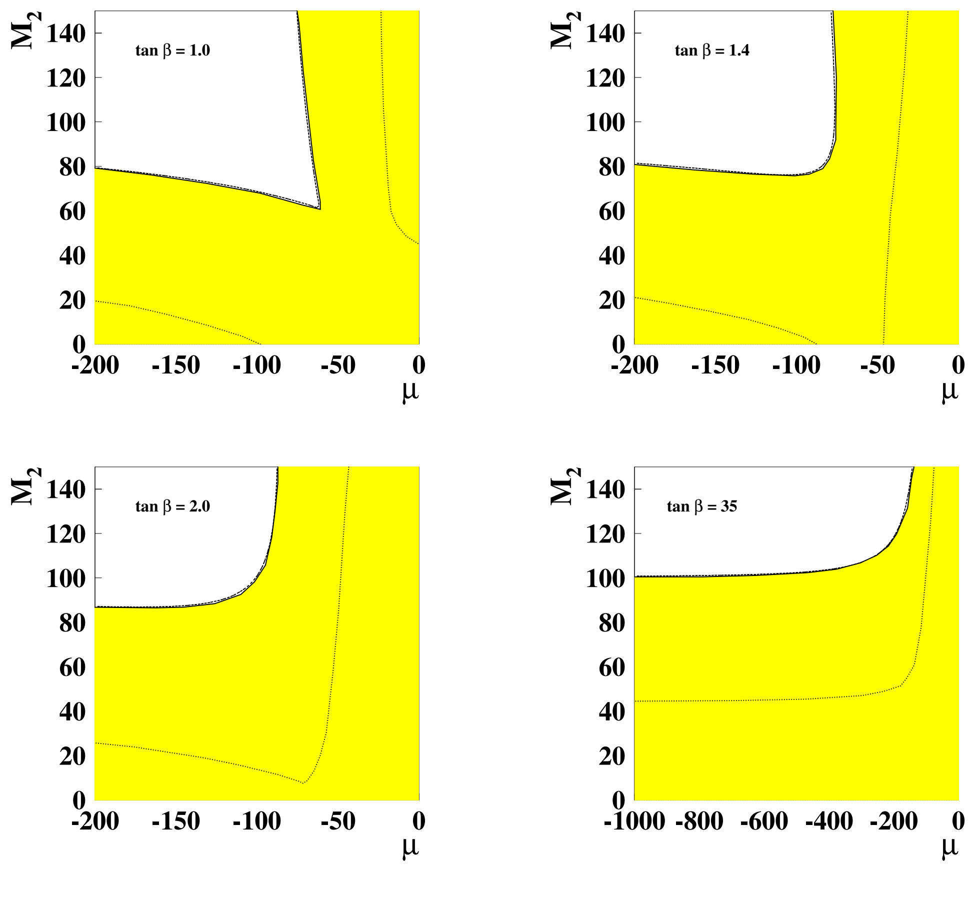

Figure 6: *Exclusion limits in the (μ, M_2)-plane for various values of* $\tan\beta$ *and for m_0=200 GeV. The excluded regions are shown for the three body chargino analysis. The LEP1 excluded regions are also indicated. The kinematic limit for chargino pair production at $\sqrt{s}$ is indicated as dashed line.*

For lower values of m_0 the coverage in the (μ, M_2) plane by chargino searches is significantly reduced. Due to the negative interference of the t-channel sneutrino exchange diagram the cross section is reduced. In addition, two body decays via sneutrinos become possible, as soon as the sneutrino becomes lighter than the chargino. In the transition region between two and three body decays appears the well known corridor in the (μ, M_2) plane. It is caused by the low efficiency for the reconstruction of two body decays with a small mass difference ΔM between the chargino and the sneutrino.

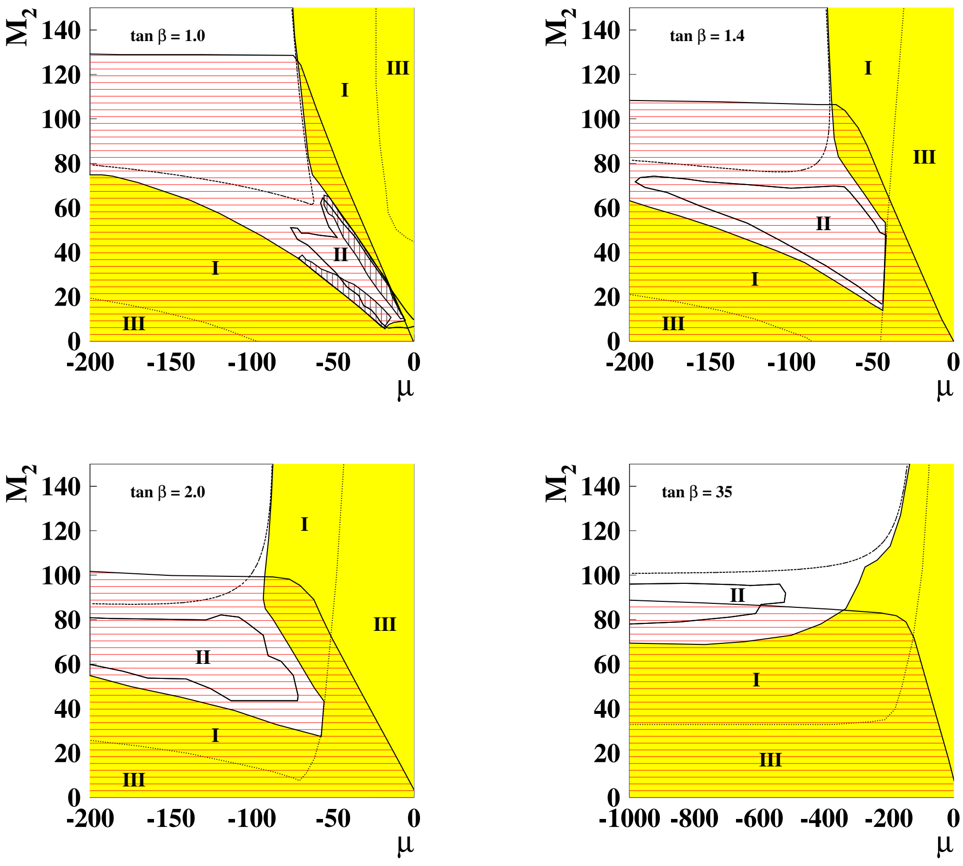

Figure 7: *Exclusion limits in the (μ, M_2)-plane for various values of* $\tan\beta$ *and for* m_0=*72 GeV. The excluded regions are shown for the individual analyses: (I) three body chargino analysis, (II) two-body chargino analysis, (III) LEP1 excluded regions, (vertically dashed) chargino decays via sleptons, (horizontally dashed) direct slepton searches.*

The results obtained for the exclusion limits in the (μ, M_2)-plane are shown in Fig.7 for a reference value of m_0= 72 GeV. Again, the results are shown for $\tan\beta$ values of 1, 1.4, 2, and 35. The various analysis contribute in different regions of parameter space: the regions marked I are excluded by three body chargino decays, the region marked II is excluded by two body chargino decays, and the regions marked III are excluded by the analysis based on the LEP-1 data. Between the regions I and II the uncovered corridor appears, due to the small efficiency of the two body analysis caused by the small mass difference between the chargino and the sneutrino.

In addition to the two- and three-body chargino analyses also the search for slepton decays of the chargino contribute to the exlusion at small values of $\tan\beta$. The region excluded is indicated as (vertically) dashed region on the plots. For a $\tan\beta$ value of 1 the corridor can be covered to a large extent by searches for chargino decays via sleptons.

These results can be directly transferred into limits on the chargino mass, as a function of $\tan\beta$ and m_0. For large m_0 values the chargino limit is found to be close to the kinematic limit for $\sqrt{s} = 202$ GeV, which is shown as dashed line on all plots. This limit deteriorates for lower values of m_0. If only chargino searches are considered, it is essentially given by the value of the sneutrino mass. This situation can be drastically improved if information from direct slepton searches is taken into account. The regions of parameter space which are excluded by selectron searches are indicated on the plots as the (horizontally) dashed areas.

4 Effects of stau mixing

In the following the effects of stau mixing on the chargino limits are investigated. The mixing can be controlled by the parameter A_τ which appears in the off-diagonal matrix elements of the stau mass matrix. In all cases considered so far, this parameter has been chosen to be $A_\tau = \mu\tan\beta$ such that no mixing effects between the right and left-handed stau are present.

An alternative way to control the stau mixing is to use a mixing angle φ_τ instead. This mixing angle is introduced in the usual way, i.e. the sine and cosine of this angle are used as elements of a unitary matrix U, needed to diagonalize the stau mass matrix. The relation between the parameter A_τ and φ_τ is given by:

$$A_\tau = \mu\tan\beta \; + \; \frac{1}{2}\tan(2\varphi_\tau)\left(\frac{m^2_{\tilde{\tau}_R} - m^2_{\tilde{\tau}_L}}{m_\tau}\right)$$

The case $\varphi_\tau = 0$, corresponds to the no-mixing case, for which the relation $A_\tau = \mu\tan\beta$ is fulfilled. In the MSSM with GUT relations the right handed stau appears to be the lighter one of the the two staus. If the mixing is increased, i.e. for increasing values of the mixing angle, the lighter stau, the $\tilde{\tau}_1$, becomes an admixture of the left-handed stau, until for a mixing angle of 45° maximal mixing is reached. In this case the right and left-handed components of the $\tilde{\tau}_1$ are equal. However, already for smaller values of the mixing angle, which are still close to 45°, the $\tilde{\tau}_1$ becomes the lightest SUSY particle. This case of the stau-LSP is not further considered in the present analysis. In principle also mixing angles above 45° can be considered. In this case the role of the left and right handed components has been exchanged, for a mixing angle of 90°, for example, the $\tilde{\tau}_1$ is completely left-handed.

The dependence of the stau masses and of the branching ratios on the mixing angle φ_τ are illustrated in Fig.8 for a point in the deep gaugino region. A point with parameters $\mu = -500$ GeV, $M_2 = 60$ GeV, $\tan\beta = 1.4$ and $m_0 = 48$ GeV has been chosen. In addition to the stau masses also the masses of the chargino, of the lightest neutralino, and of the sneutrino are indicated. At this point in parameter space, the $\tilde{\tau}_1$ becomes the lightest SUSY particle for mixing angles around 37°. In part b) of the figure the branching ratios of the chargino in the various decay channels (3-body W^* decay, slepton decays (sl) and 2 body decay via a sneutrino (2b)) are shown as a function of the mixing angle. Since for this point in parameter space the two-body chargino decays are open, the contribution of the three-body decays is very small. In the no-mixing case the chargino decays to nearly 100% into a sneutrino (two-body decay). With increasing mixing the $\tilde{\tau}_1$ develops a left-handed component and decays into staus become possible. Their fraction increases up to the point where the $\tilde{\tau}_1$ becomes the LSP. For the corresponding mixing angles above 45° the branching ratio into $\tilde{\tau}_1$ is higher since for the same mass there is a larger left handed component. For all mixing angles up to 90° the branching ratio for chargino decays into the lightest stau stays at a sizeable fraction. The fraction P_τ of the leptonic chargino decays (W^* and slepton decays) into taus is plotted in part c) of the figure. For mixing angles below 45° it raises from a value of 33% to nearly 100%, for mixing angles above 45° only decays into the left handed staus are possible such that P_τ remains 100%.

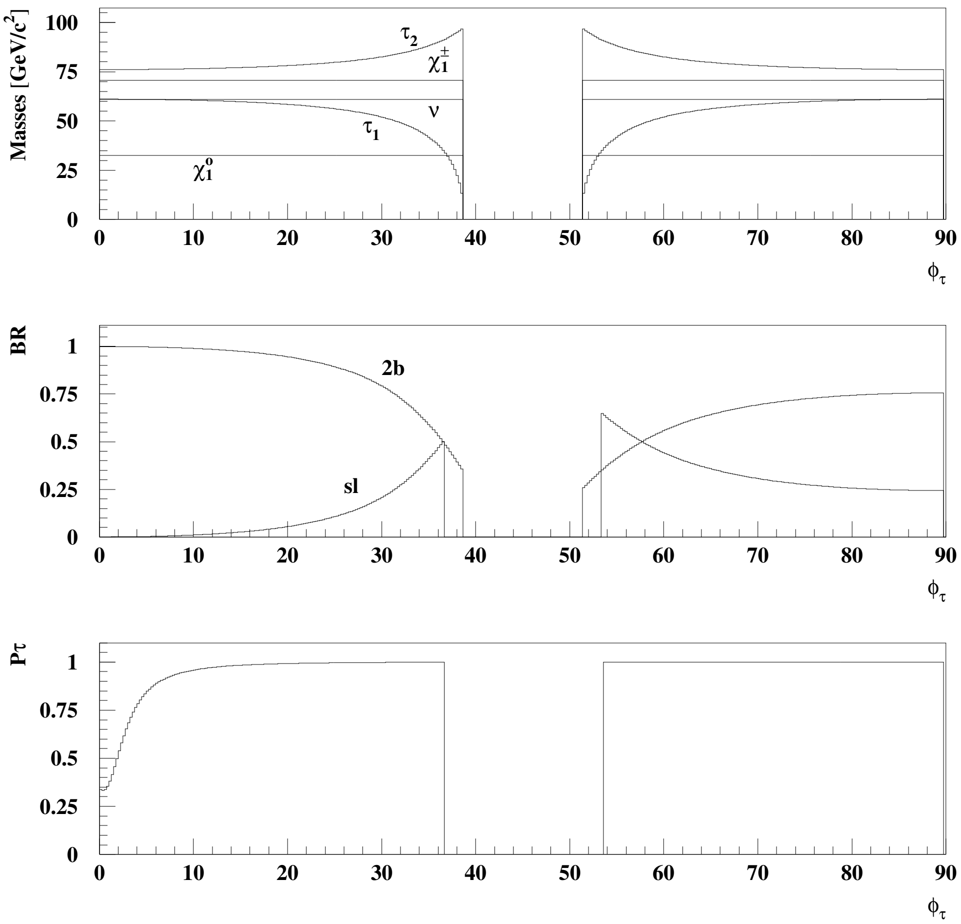

Figure 8: *a) Dependence of the stau masses on the mixing angle φ_τ for a point in the deep gaugino region ($\mu = -500$ GeV, $M_2 = 60$ GeV, $\tan\beta = 1.4$ and $m_0 = 48GeV$). In addition to the stau masses also the masses of the chargino, the lightest neutralino, and sneutrinos are indicated. b) Branching ratios of the chargino into three-body W^* (not visible, since too small), two-body sneutrino decays (2b) and slepton decays (sl) as a function of the stau mixing angle φ_τ. c) The fraction P_τ of decays into taus normalized to the leptonic chargino decays (W^* and slepton decays) as a function of the stau mixing angle φ_τ.*

5 Chargino limits with stau mixing

The effects of stau mixing have been studied in the deep gaugino region for $\mu = -500$ GeV and for $\mu = -80$ GeV, for $\tan\beta$ values of 1.4 and 35. The mixing in the stop and beauty sector has been deecoupled, i.e. the values of A_t and A_b have been set to the no-mixing points. An appropriate parameter plane to study the mixing effects is the $(m_{\tilde{\nu}}, M_{\tilde{\chi}^{\pm}})$-plane, where the chargino mass is plotted versus the sneutrino mass. The corridor between two- and three-body chargino decays is visible along the diagonal in this plot. In Fig.9 the excluded regions in this plane are shown for four different values of the stau mixing angle φ_τ, for $\varphi_\tau = 0$, 25, 35 and 42 degrees for $\tan\beta = 1.4$ and $\mu = 500$ GeV. In the no-mixing case ($\varphi_\tau = 0$), the region for large $m_{\tilde{\nu}}$ is covered by the three body chargino decays via W^* (region I). The region left of the corridor for $m_{\tilde{\nu}} = m_{\chi^{\pm}}$ is covered by the two body decays (region II). For $\tan\beta$=1.4, as considered here, also a significant fraction of the plane is excluded by direct selectron searches. The corresponding region is indicated as horizontally dashed region in the plot. In particular, the full corridor region can be covered by this search. It should be noted that the shaded region in the upper left corner is either unphysical (in part of the region) or the stau appears to be the lightest SUSY particle. The border of that region is defined by the mass relation $m_{\tilde{\tau}_1} = m_{\chi^0}$.

As already expected from the branching ratios and mass relations shown in Fig.8, mixing effects become only important for mixing angles above $\sim 30°$. For such large angles the slepton decays contribute significantly. The region of parameter space which can excluded by chargino decays via sleptons is indicated as vertically dashed region in the plots. Both the three- and the two-body exclusion regions become smaller with increasing mixing, whereas the region excluded by chargino decays into sleptons becomes larger. Although it covers part of the corridor between the mass denerate chargino and sneutrino line, there is a net loss, since the efficiency for the stau selection is lower than for the three- and two-body selections. For extreme mixing angles beyond 40 degrees the two body chargino decays have disappeared.

It is important to note that with increasing mixing angle the lightest stau becomes the LSP over a significant fraction of the parameter space. In this scenario a new corridor opens up. The present tau searches are not sensitive if the mass difference of the stau to the neutralino is small or if the stau does not decay any longer into the neutralino. This happens if the mass difference between the stau and the neutralino is smaller than $\sim$1.8 GeV such that deacys of the type $\tilde{\tau} \to \chi^0\tau$ are kinematically forbidden. At small mixing angle this corridor is not visible, since two body decays are still possible and the mass difference ΔM in the the chargino decay to staus is larger. The only other channel considered so far which has sensitivity in this corridor region is the direct search for selectrons. Since for large mixing angles the new corridor appears at small values of $m_{\chi^{\pm}}$, the coverage of the direct slepton searches is limited and chargino mass limits can only be placed at relatively low mass values.

The exclusion of the direct slepton search is even less powerful for large values of $\tan\beta$. This can be seen in the comparison of Figs.9 and 10. In Fig.10 the same plots as discussed previously are shown for $\tan\beta$=35 instead of $\tan\beta$=1.4. For this large values of $\tan\beta$ the selectron exclusion corresponds to smaller values of $m_{\tilde{\nu}}$. Therefore the new corridor in the region where the $\tilde{\tau}$ becomes mass degenerate with the neutralino is even less covered than for small $\tan\beta$ values. If this corridor cannot be covered by another independent analysis, stau mixing effects at large $\tan\beta$ will affect the absolute limits on the masses of charginos and neutralinos. Therefore a dedicated search for a single tau topology has been started to address this problem. Since for the same values of $m_{\tilde{\nu}}$ and $m_{\chi^{\pm}}$ sleptons are heavier at large $\tan\beta$ values as compared to small $\tan\beta$ values, the contributions from the slepton decays of charginos only contribute for large mixing angles.

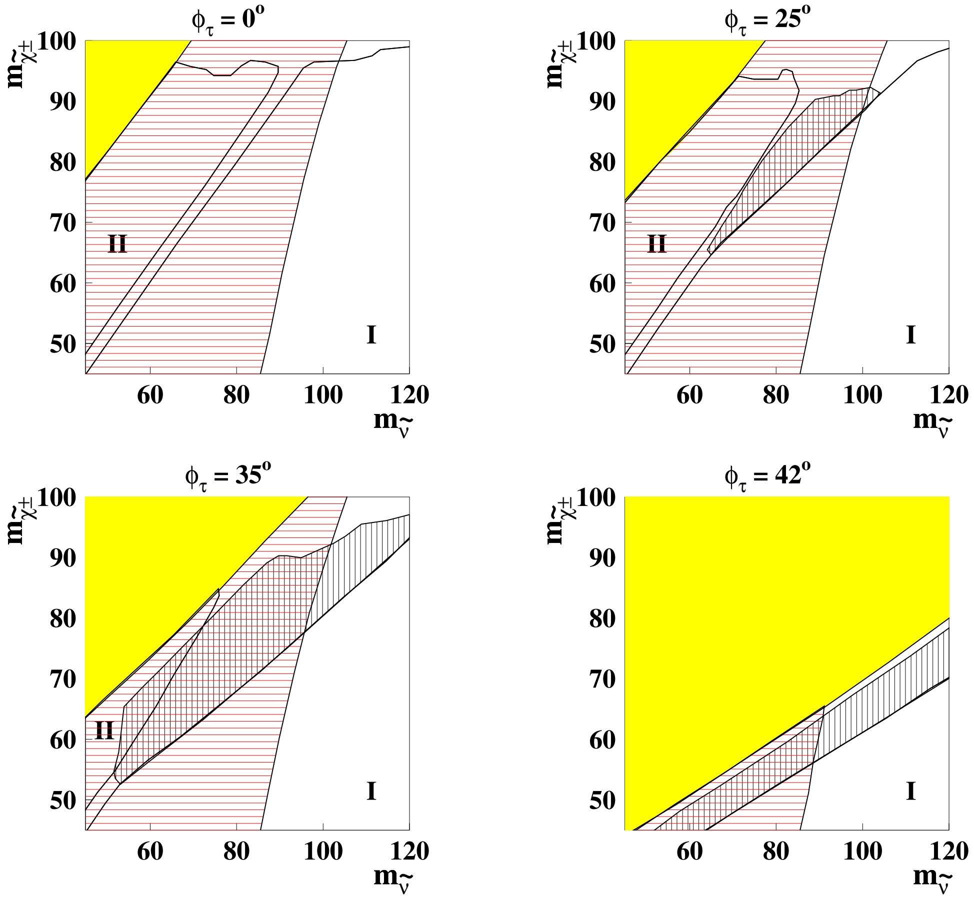

Figure 9: *Limits in the* $(m_{\tilde{\nu}}, M_{\tilde{\chi}^{\pm}})$*-plane for a point in the gaugino region* ($\mu = -500$ *GeV) for* $\tan\beta = 1.4$ *for various stau mixing angles* φ_τ.

In the region around μ=-80 GeV the mixing effects are less strong. This is illustrated in Fig.11, where the corresponding plots are shown for $\mu = -80$ GeV and $\tan\beta$=1.4.

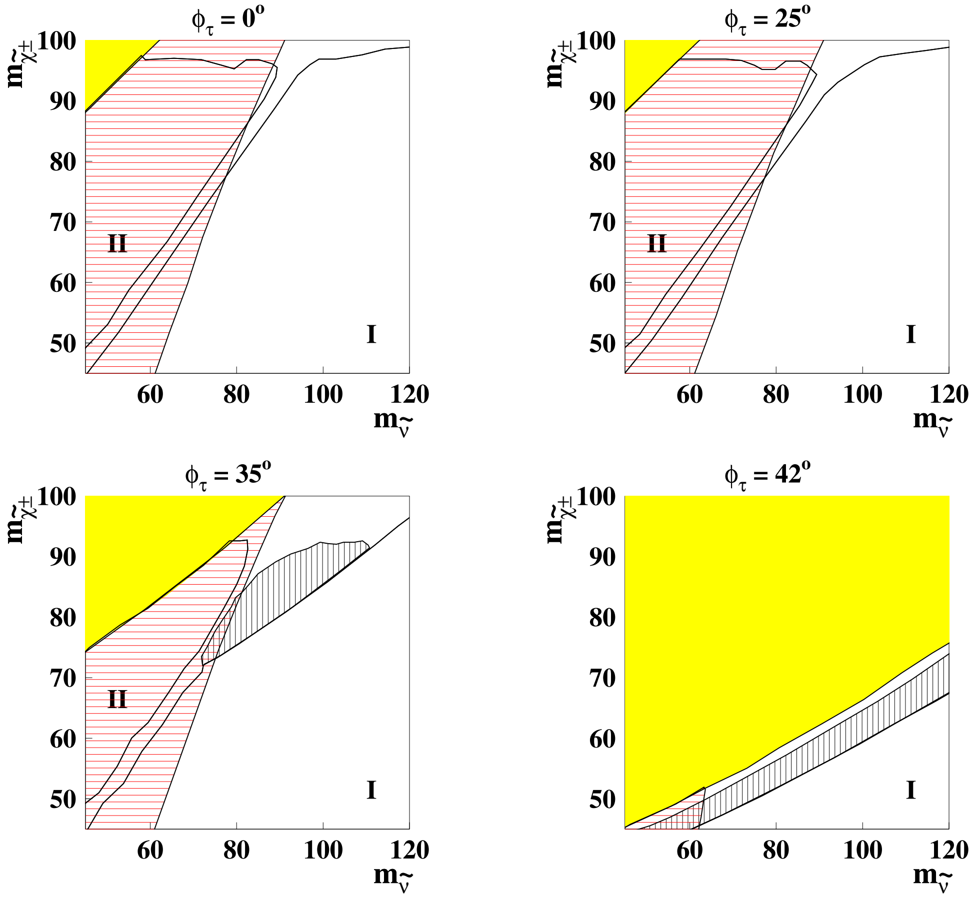

Figure 10: *Same as Fig.9, but for* $\tan\beta = 35$*.*

The same qualitative behaviour as seen before is found. With increasing mixing both the covered two and three body regions are reduced. Some of the parameter space can be recovered by chargino decays to sleptons/staus. As in the deep gaugino region, the effects for the chargino limit are most significant for large mixing angle. In this mixed region the stau LSP corridor appears however at larger values of the chargino mass.

The studies performed so far can be used to extract a limit on the chargino mass as a function of the stau mixing angle. For small mixing angles the limit is set at the border between the region excluded by three body chargino decays and the region excluded by a direct slepton search. For increasing mixing the limit deteriorates since the region excluded by three body decays is reduced. For extreme mixing angles the chargino limit is set in the new stau-LSP corridor where the stau mass approaches the neutralino mass. The results are summarized in Fig.12, where the limit on the chargino mass is plotted as a function of the stau mixing angle φ_τ. Curves are shown for different μ and $\tan\beta$ values. The limit has been determined including the

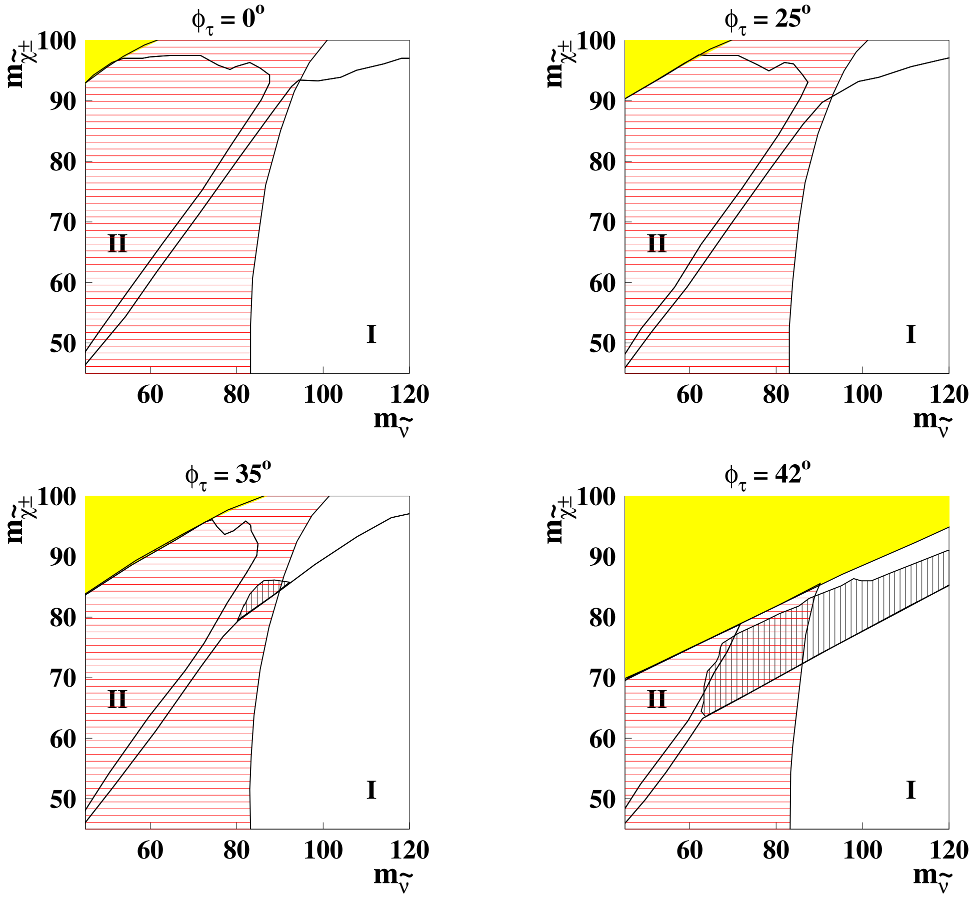

Figure 11: *Limits in the* $(m_{\tilde{\nu}}, M_{\tilde{\chi}^\pm})$*-plane for* $\mu = -80$ *GeV and* $\tan\beta = 1.4$ *for various stau mixing angles* φ_τ.

full information from the three- and two-body analyses, from the chargino decays via sleptons and from the direct selectron searches. The general trend is that the chargino limit is relatively stable up to mixing angles around 35 degrees. Beyond that there is a drastic decrease due to the fast changing $\tilde{\tau}_1$ mass and the appearing stau-LSP channel. It is important that this channel is covered by additional analyses searching for a single tau topology with or without a long living stau.

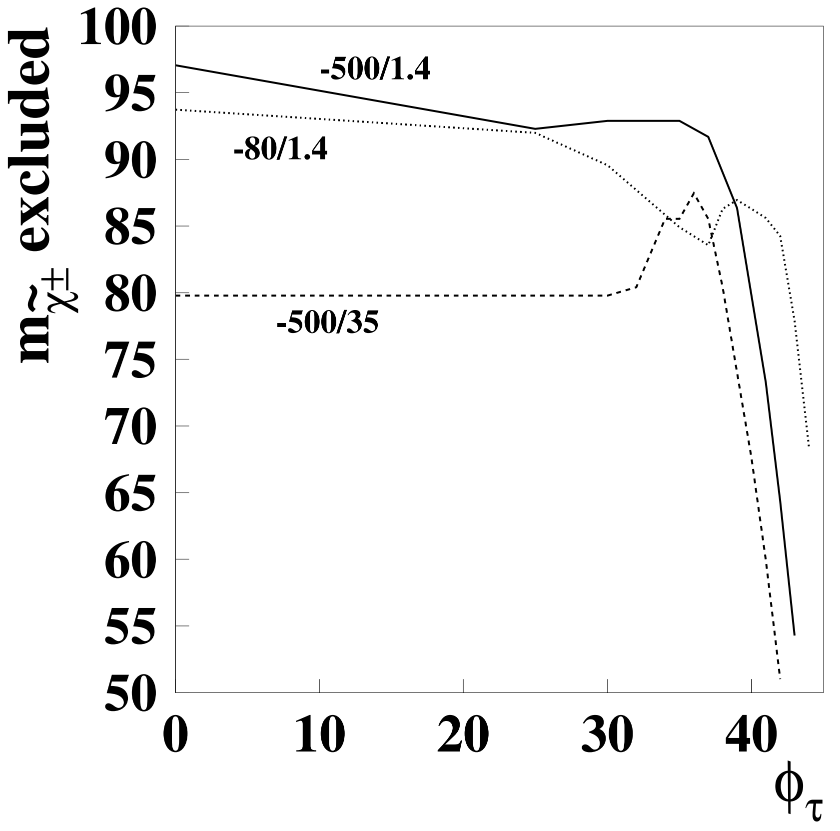

Figure 12: *Limits on the chargino mass for various μ and $\tan\beta$ values as a function of the mixing angle φ_τ.*

The present analysis has also been extended for stau mixing angles beyond 45 degrees. The corresponding results are shown in Fig.13 for μ=-500 GeV, $\tan\beta$=1.4 and mixing angles φ_τ of 48, 55, 65 and 90 degrees. These angles have been chosen to be symmetric around 45° to the ones shown in Fig.9. For mixing angles close

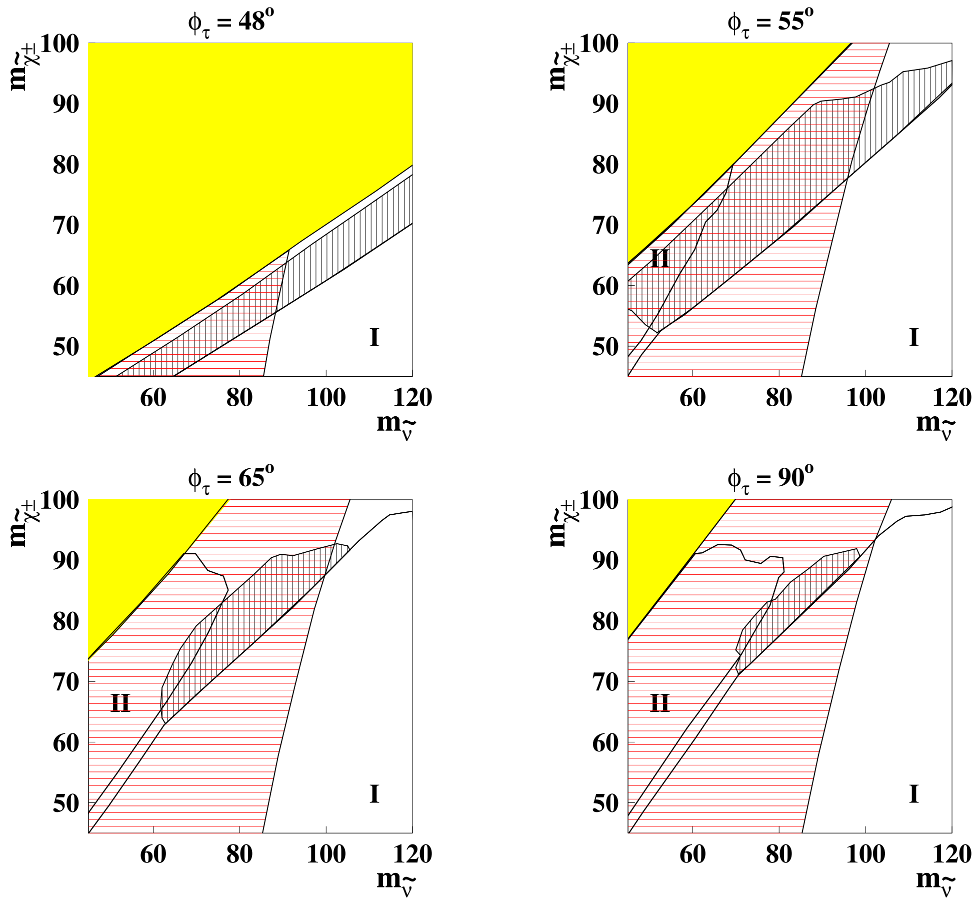

Figure 13: *Limits in the* $(m_{\tilde{\nu}}, M_{\tilde{\chi}^\pm})$*-plane for a point in the gaugino region* ($\mu = -500$ *GeV) for* $\tan\beta = 1.4$ *for stau mixing angles* φ_τ *larger than 45°.*

to 45° the excluded regions are similar to those found for the corresponding mixing angle below 45°. For large mixing angles, approaching 90°, the coverage from the slepton decays of the charginos is larger, since the lightest stau is left handed.

6 Conclusions

The impact of stau mixing on the chargino limits has been studied using the ALEPH data collected at various centre-of-mass energies between 189 and 202 GeV. It has been found that the chargino mass limits are seriously affected if large mixing effects are present. The principle problem is an uncovered region which appears if, due to mixing, the mass of the lightest stau approaches the mass of the lightest neutralino. So far this region is only covered by direct slepton searches. For large mixing angles these searches exclude however only a small part of the uncovered region at relatively small values of $m_{\chi^\pm}$ and $m_{\tilde{\nu}}$. In order to improve the situation a dedicated new analysis is needed in which a search for a single tau with or without a long living stau is performed.

References

[1] T. Neunhöffer, *Suche nach leptonischen Charginozerfällen unter Berücksichtigung der Stau-Mischung in e^+e^--Kollisionen mit dem ALEPH-Detektor*, Diploma thesis, Mainz 1999.

[2] H.A.Nürnberger, *Suche nach leptonischen Charginozerfällen in e^+e^--Kollisionen bei Schwerpunktsenergien bis 189 GeV und Bestimmung einer Neutralinomassengrenze*, PhD thesis, Mainz (1999).

[3] ALEPH Collaboration, *Searches for chargions and neutralinos in e^+e^- collisions at $\sqrt{s}$ = 161 and 172 GeV*, CERN-PPE/97-128 (1997).

[4] ALEPH Collaboration, *Search for chargions and neutralinos in e^+e^- collisions at centre-of-mass energies near 183 GeV and constraints on the MSSM parameter space*, CERN-EP/99-014 (1999).

[5] P.Azzouri, private communication.

[6] W.J. Stirling, J.Phys. G17 (1997), 1567.